

# THE EFFECT OF SECONDARY HARDENING ON THE FRACTURE TOUGHNESS OF A BAINITIC MICROSTRUCTURE

**H. Kotilainen**

**Technical Research Centre of Finland, SF-02150 Espoo 15, Finland**

## ABSTRACT

A bainitic Cr-Mo-V alloyed pressure vessel steel in three heat treatment conditions has been investigated. The effective grain size e.g. the bainitic packet size is not sensitive to the heat treatment whereas the size and distribution of the carbides and the dislocation density vary with tempering. The yield strength and the cleavage fracture strength has been shown to depend on the dislocation density, but the fracture process is controlled by the bainite packet boundaries. The cleavage fracture strength can be divided into two parts, the tensile or macroscopical and the microscopical one. In certain cases when the strain hardening is large enough a yield controlled cleavage fracture strength can be found. The fracture facets are of the same size as the bainite packet. The characteristic distance is dependent on the cleavage fracture strength and it is several times larger than the bainite packet. Using a model of the temperature dependence of the fracture toughness the toughness has been expressed as a function of the average mesh length of the dislocation network.

## KEYWORDS

Fracture toughness; bainite; carbides; microstructure.

## INTRODUCTION

The effect of small precipitates on toughness has not been very extensively studied and the results are contradictory (Ritchie and co-workers, 1979; Nakazawa and Krauss, 1978).

Weak dislocation obstacles were found to be detrimental to the toughness (Hahn and Rosenfield, 1966a). However, if strong obstacles are small enough, they can raise the resistance to brittle fracture. This is due to the fact that the dislocation pile-ups then became shorter and their length approaches the interparticle distance. The formation of dislocation pile-ups can be even prevented and the small particles cause more homogeneous deformation (Tanaka and co-workers, 1975; Naylor, 1979) and thus they are advantageous to the toughness (Roesch, 1973; Kamada and co-workers, 1976).

Carbide distribution or dislocation density is only seldom considered in relation to the fracture toughness. In the following, attention is paid to a bainitic steel in three heat treatment conditions, in which the bainitic packet size remains constant, but the amount of carbides and the dislocation density have been varied.

### RESULTS

The material studied was a bainitic Cr-Mo-V alloyed steel with 0.16 % C, 2.8 % Cr, 0.6 % Mo and 0.3 % V. The heat treatment was a quench and temper simulating the cooling of a thick plate. Three different heat treatments 940°C/5 h/600°C/20 h, 980°C/6 h/670°C/20 h and 980°C/6 h/760°C/20 h were used (Törrönen, 1979). In the following these different heat treatments are identified with M, T and K, respectively. These heat treatments correspond to the tempering parameters 18650 (M), 20100 (T) and 22000 (K). In Fig. 1 the respective yield strength values are given. Figure 1 shows how the heat treatments are located on the tempering curve (Törrönen, 1979). Figure 2 shows the distribution of the small vanadium carbides in heat treatment condition T.

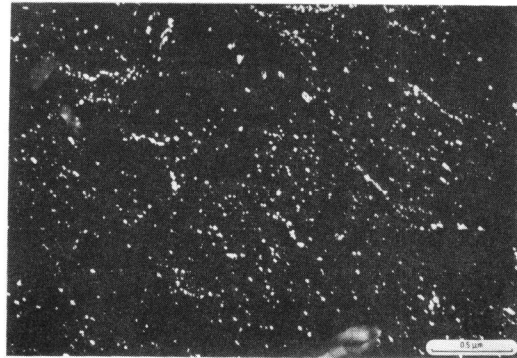
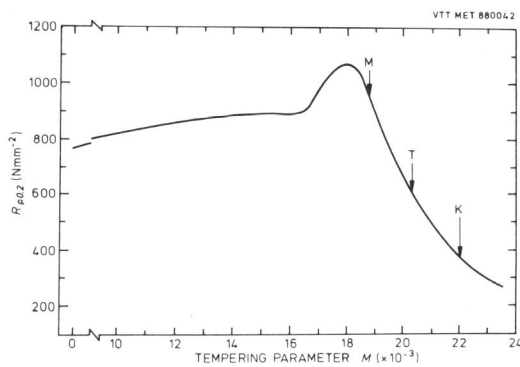


Fig. 1. Room temperature tensile yield strength as a function of the tempering parameter.

Fig. 2. Vanadium carbides in heat treatment condition T.

Four different grain size units must be considered. The prior austenite grain size is divided into packet bundles, which are composed of parallel packets. The packets are the smallest units surrounded by high angle boundaries. The packet size is not dependent on the prior austenite grain size. The packets are further divided into parallel laths and/or cells. The size and distribution of the MC-type carbides are both strongly dependent on the heat treatment. The microstructural units are given in Table 1 (Törrönen, 1979).

TABLE 1 Microstructural units for the heat treatment conditions K, T and M.

Unit	Heat treatment condition		
	K	T	M
Prior austenite grain ( $\mu\text{m}$ )	110	115	50
Packet (mean) ( $\mu\text{m}$ )	3.0	3.0	3.0
Mean caliber diameter of the MC-type carbide (nm)	43.3	14.2	5.5
Planar interparticle spacing (nm)	466	131	51
Mesh length of dislocation network (nm)	135	82	49
Dislocation density ( $\times 10^{-10} \text{cm}^{-2}$ )	2	6	16

Tensile tests were performed in the temperature range 12-300 K to establish the temperature dependence of the yield strength. The yield strength was taken to be the lower yield strength value or the 0.2 % proof strength. The results are given in Fig. 3 for all three heat treatment conditions.

The fracture toughness  $K_{IC}$  has been measured using 25 mm thick CT and 3-point bend specimens and one 75 mm thick specimen. Valid  $K_{IC}$  values were measured up to 185 K, and these values are denoted in Fig. 4 with filled points. The  $K_{IC}$  versus temperature curve has been estimated between the temperatures 185 K and 260 K using the J-integral calculation method reported by Chell and Milne (1976). The points at 77 K were not valid because of the too high precracking load. However, this is not thought to seriously affect the results. All specimens up to 260 K showed a cleavage type fracture.

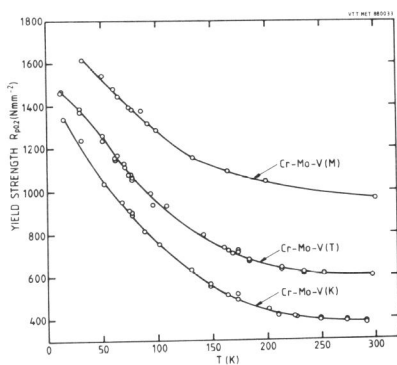


Fig. 3. The temperature dependence of the yield strength for heat treatment conditions K, T and M.

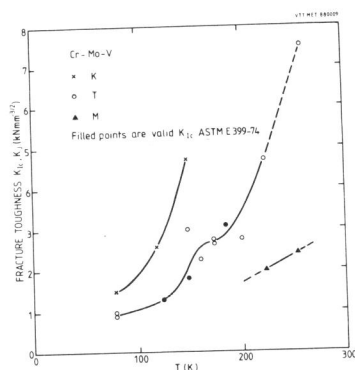


Fig. 4. Fracture toughness for the heat treatment conditions K, T and M.

## DISCUSSION

### Cleavage Fracture Strength

To separate the temperature dependent component of the yield strength from the temperature independent component, a function given in Eq. (1) was used (Yaroshevich and Ryvkina, 1970)

$$\sigma_Y = \sigma_\mu + (\sigma_0 - \sigma_\mu) \exp(-mT) \quad (1)$$

in which  $\sigma_Y$  is the yield strength,  $\sigma_\mu$  is the temperature independent component of the yield strength,  $\sigma_0$  is the yield strength at 0 K,  $m$  is a constant and  $T$  is the temperature. The constants in Eq. (1) are given in Table 2 for the three heat treatment conditions.

TABLE 2 The temperature dependence of the yield strength

Condition	$\sigma_\mu$ (Nmm <sup>-2</sup> )	$\sigma_0$ (Nmm <sup>-2</sup> )	$m$ (K <sup>-1</sup> )	Temperature range (K)
K	285	1640	0.0104	31 < T < 248
T	500	1755	0.0104	30 < T < 233
M	905	1955	0.0104	17 < T < 199

Following the idea of Wobst and Aurich (1977), the value of  $\sigma_0$  can be interpreted as the cleavage fracture strength  $\sigma_{fc}$ . This idea holds for the uniaxial tension case and for blunt notch specimens (Kotilainen, 1980). The  $\sigma_{fc}$  value has to be distinguished from the microscopical cleavage fracture strength  $\sigma_f^*$ , which was established by Tetelman and co-workers (1968). If a limiting notch root radius  $\rho_0$  characteristic for the material in question exists, then the fracture toughness  $K_{IC}$  can be given (Malkin and Tetelman, 1971)

$$K_{IC} = 2.9\sigma_Y [\exp(\sigma_f^*/\sigma_Y - 1) - 1]^{1/2} \sqrt{\rho_0} \quad (2)$$

Using the value of  $\rho_0 = 14 \mu\text{m}$  according to Kotilainen and co-workers (1980) the fracture toughness (Fig. 4) and the yield strength (Fig. 3), Eq. (2) can be applied for the estimation of the microscopical cleavage fracture strength. The calculation shows that the cleavage fracture strength increases with decreasing temperature for the condition T, but approaches a fairly constant value of 3000 Nmm<sup>-2</sup> at low temperatures. The calculation is not performed for the conditions M and K because there is not sufficient fracture toughness data. If the limiting notch root radius is characteristic for the material and can be related to the grain size as predicted by Malkin and Tetelman (1971), the calculated microscopical cleavage fracture strength should also apply to the heat treatment conditions M and K. However,  $\sigma_0$  measured in the tensile test is definitely different for the different conditions K, T and M.

Another approach to estimate the cleavage fracture strength is to use the result of Rice and Rosengren (1968) for calculating the maximum stress in front of a crack as a function of the strain hardening exponent. In Fig. 5 the strain hardening exponent calculated by means of the tensile test data is given. Performing the calculation and putting the peak stress at the crack tip equal to the cleavage fracture strength, continuously increasing strength values with decreasing temperature are found. At low temperatures (< 100 K) a fairly constant value given in Table 3 is achieved for each heat treatment condition.

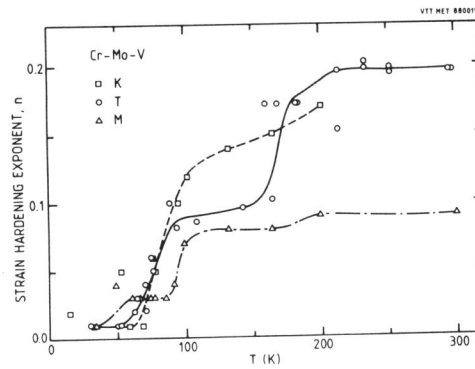


Fig. 5. Calculated strain hardening exponent as a function of temperature.

TABLE 3 Estimated cleavage fracture strength for the different heat treatment conditions.

Condition	Cleavage fracture strength ( $\text{Nmm}^{-2}$ )
K	2550
T	3015
M	3650

For the heat treatment condition T a fairly constant value of  $2550 \text{ Nmm}^{-2}$  for the calculated stress has also been found at intermediate temperatures (120–240 K). The same value can be found using Eq. (2) if  $\rho_0$  is equal to  $30 \mu\text{m}$ . This constant value is due to the rapid increase of the strain hardening, which in the specific temperature range is able to compensate the drop of the yield strength. This behaviour is not observed in other materials, because in condition K the drop of the yield strength with increasing temperature is so large that the strain hardening cannot compensate it. In condition M the strain hardening is so low that the drop of the yield strength is not compensated.

Therefore the intermediate value of  $2550 \text{ Nmm}^{-2}$  can be interpreted as a microscopical cleavage fracture strength in yield controlled fracture, whereas the low temperature values of Table 3 are microscopical cleavage fracture strengths in a mechanism controlled fracture. Consequently the cleavage fracture of the heat treatment condition K at all temperatures is yield controlled, whereas the cleavage fracture of the heat treatment condition M is always controlled by the mechanism. The cleavage fracture strength can also be estimated using the Griffith-Orowan equation

$$\sigma_{fc} = \left[ \frac{2E \gamma_p}{(1-\nu^2)\pi a} \right]^{1/2} \quad (3)$$

where E is Young's modulus,  $\gamma_p$  the effective surface energy and 2a the crack length. If the crack length is equal to the mean fracture facet size ( $3.6 \mu\text{m}$ ) (Kotilainen, 1980), which in turn is equal to the bainitic packet size, and the effective surface energy is chosen equal to  $120 \text{ Jm}^{-2}$  (Brozzo and co-workers, 1977; Roman and co-workers, 1979), the cleavage fracture strength of  $3100 \text{ Nmm}^{-2}$  is found. This value corresponds well to the estimated cleavage fracture strength for the condition T given in Table 3. For conditions K and M the Griffith-Orowan equation gives approximately the same value for the cleavage fracture strength because the size of the fracture facet is almost constant.

The cleavage fracture strength can now be correlated to the microstructure. The packet size cannot be considered, because it does not change between the different heat treatments. The yield strength  $\sigma_0$  at 0 K can be interpreted as the maximum cleavage fracture strength in a uniaxial tension test,  $\sigma_{fcmax}$ . Therefore it can be correlated to the same factors which determine the yield strength i.e. the small carbides and the dislocation density. In Fig. 6 a  $\sigma_{fcmax}$  is plotted against the dislocation density  $\rho_d$  and the average mesh length of dislocation network  $L_m$ . In Fig. 6 b the microscopical cleavage fracture strength is also given as a function of the dislocation density  $\rho_d$ , and of the mesh length  $L_m$ .

A fairly linear dependence is found for both variables. Therefore it seems reasonable that the cleavage fracture strength is related to the dislocation density as found by Groom and Knott (1975) in the case of cold worked material. The inverse of the mesh length of dislocation network is related to the square root of the dislocation density. According to this, the slightly nonlinear dependence between  $\sigma_f^*$  and  $L_m$  is predictable. The physical meaning of the cleavage fracture strength cannot be explained by the microstructural dependence. However, this dependence can be used for design of alloys, although it must be realized that a high value of the cleavage fracture strength does not necessarily result in high toughness.

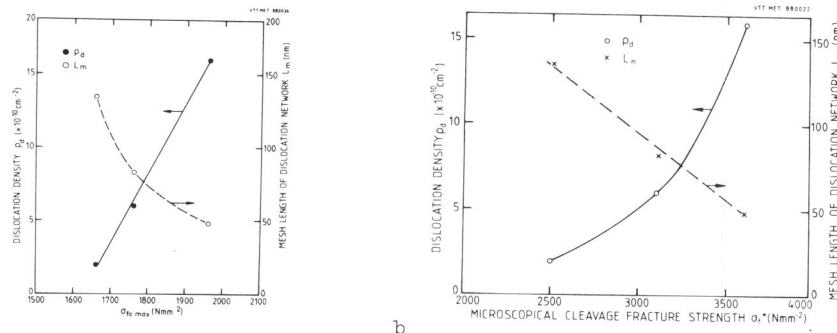


Fig. 6. Cleavage fracture strength as a function of the dislocation density and of the mesh length of dislocation network a) tensile cleavage fracture strength  $\sigma_{fcmax}$ , b) microscopical cleavage fracture strength  $\sigma_f^*$ .

#### The Characteristic Distance

Ritchie and co-workers (1973) introduced the idea of the characteristic distance over which the stress has to exceed the cleavage fracture strength to obtain fracture. The characteristic distance can be calculated by means of the stress distributions of Rice and Johnson (1970) and Tracey (1976) for a blunted crack and for a sharp crack, respectively. However, if  $\sigma_{fcmax}$  is used for the cleavage fracture strength, the characteristic distance is not constant but increases with increasing temperature (Fig. 7a) (Kotilainen, 1979). This is probably due to the low stress concentration which in turn leads to very large distances ahead of the crack tip - larger than the plastic zone. Therefore, the stress distributions are no longer valid and the calculation of the characteristic distance fails. By using the microscopical cleavage fracture strength given in Table 3, estimates for the characteristic distance can be made. The result of the calculation is given in Fig. 7b. The calculation has been performed using the actual strain hardening exponent (Fig. 5) and both Rice-Johnson's and Tracey's stress distributions. For comparison the characteristic distance calculated from the value  $\sigma_{fc} = 2550 \text{ Nmm}^{-2}$  is also given. The characteristic distances according to Fig. 7 are given in Table 4 for the heat treatment condition T.

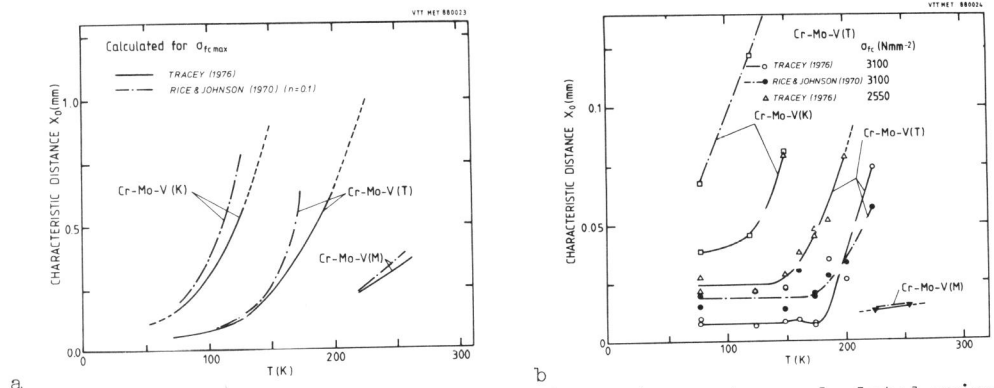


Fig. 7. Characteristic distance as a function of temperature calculated using different values of the cleavage fracture strength. a)  $\sigma_{fcmax}$  b)  $\sigma_f^*$

TABLE 4 Characteristic distance  $X_0$  of the heat treatment condition T.

Stress distribution	$\sigma_{fc}$ (Nmm <sup>-2</sup> )	$X_0$ ( $\mu$ m)
Rice-Johnson	3100	19
Tracey	2550	25
Tracey	3100	8
Tracey	1755	65

For the condition K no constant value can be found and for the condition M there is not enough data for carrying out the calculation. However, the tendency is quite clear that with increasing cleavage fracture strength the characteristic distance decreases. According to Table 4 and Table 1 the characteristic distance varies between 2.7  $d_p$  and 8.3  $d_p$ , if  $d_p$  is the bainitic packet size. These values correspond well with the literature data but are, however, slightly larger. Therefore, it can be assumed that in a bainitic packet structure with high dislocation density more microstructural units are involved in the fracture process than in mild steel. This is consistent with the observation that in a structure with high dislocation density the yielding of numerous small units results in the same effect as the yielding of few grains. Assuming that all the carbides are nucleated on the dislocations, the average length between carbides along the dislocation line can be obtained by dividing the dislocation density by the carbide density. This gives a value 146 nm for the condition T, whereas the average mesh length is 82 nm according to Table 1 (Törrönen, 1979). A vanadium-rich carbide is on the average found on 2/3 of the dislocation nodes and the critical radius of a dislocation source is a half of the mesh length. Using this knowledge Törrönen (1979) has calculated the number of operating dislocation sources of  $1.5 \cdot 10^{15} \text{ cm}^{-3}$ . However, if the number of possible dislocation sources S is estimated according to Eq. (4)

$$S = \frac{\rho_d}{L_m} \quad (4)$$

the result is  $7.4 \cdot 10^{15} \text{ cm}^{-3}$ . This result indicates that on average every fifth source is operating. Further, this result clearly shows that to obtain the plastic deformation needed for yielding it is necessary and sufficient that the operating sources generate only one dislocation. Thus it is unlikely that any pile-up formation occurs upon initial yielding. The result can also be interpreted so that

the vanadium-rich carbides have no direct influence on the dislocation movement upon initial yielding. They have, however, an indirect influence by stabilizing the dislocation structure during tempering.

### Microstructure and Fracture Toughness

An inverse relationship between the fracture toughness and the yield strength has been reported by numerous authors (Irwin and co-workers, 1967; Hahn and Rosenfield, 1966b). These observations are mostly experimental in nature and therefore the applicability of the models may be restricted to the materials investigated. But relating the fracture toughness to the yield processes in a fracture process volume inside the plastic zone, the fracture toughness can be given as a function of the temperature dependent and independent components of the yield strength (Kotilainen, 1979)

$$K_{Ic} = A + k \frac{\sigma_Y}{\sigma_\theta}, \quad (5)$$

where  $\sigma_\theta$  is the temperature dependent component of the yield strength and A and k are constants. The temperature independent component  $\sigma_\mu$  can be given (Törrönen, 1979)

$$\sigma_\mu = \alpha G b L_m^{-1} \quad (6)$$

where  $\alpha$  is a constant, G is the shear modulus and b is the Burgers vector. The temperature dependent component is according to Eq. (1)

$$\sigma_\theta = (\sigma_o - \sigma_\mu) e^{-mT} \quad (7)$$

Combining Eqs. (5), (6) and (7) the fracture toughness can be expressed

$$K_{Ic} = A + k \left[ \left( \frac{\sigma_o L_m}{\alpha G b} - 1 \right)^{-1} e^{mT} + 1 \right] \quad (8)$$

Eq. (8) gives the relationship between the dislocation density and fracture toughness. An increase of the mesh length has been shown to decrease the cleavage fracture strength (Fig. 6). Considering  $\sigma_o$  and  $\sigma_\mu$  (Table 2), Eq. (8) predicts that the fracture toughness increases as the mesh length increases. This behaviour is qualitatively shown in Fig. 4, because the mesh length increases as the tempering temperature increases (see Table 1).

The fracture toughness (the initiation of fracture) and the yield strength are controlled by the dislocation density. It is assumed that the constant k includes the cleavage fracture strength and probably strain hardening. Dislocation tangles and low angle boundaries do not resist the crack nucleus, but the first strong barrier is the high angle packet boundary, which control the crack propagation (Kotilainen and co-workers, 1980).

### CONCLUSIONS

The cleavage fracture strength and the initiation fracture toughness have been shown to be controlled by the mesh length of the dislocation network or equivalently the dislocation density in a bainitic microstructure. The cleavage fracture strength can be estimated by means of low temperature tensile tests, but this result must be separated from the microscopical cleavage fracture strength which



is much higher. The characteristic distance depends on the value of the cleavage fracture strength and does not correspond to any microstructural unit. It is about 3 to 8 times larger than the bainitic packet size or the fracture facet size.

## REFERENCES

- Brozzo, P., G. Buzzichelli, A. Mascanzoni, and M. Mirabile (1977). Microstructure and cleavage resistance of low-carbon bainitic steels. Met. Sci., 11, 123-129.
- Chell, G. G., and I. Milne (1976). A new approach to the analysis of invalid fracture toughness data. Mat. Sci. Eng., 22, 249-253.
- Groom, J. D. G., and J. F. Knott (1975). Cleavage fracture in prestrained mild steel. Met. Sci., 9, 390-400.
- Hahn, G. T., and A. R. Rosenfield (1966a). A modified double-pile-up treatment of the influence of grain size and dispersed particles on brittle fracture. Acta Met., 14, 1815-1825.
- Hahn, G. T., and A. R. Rosenfield (1966b). Mechanics and metallurgy of brittle crack extension. Proc. of the ASCE Engineering Mechanics Division Specialty Conference (Washington D.C.), 351-383.
- Irwin, G. R., J. M. Krafft, P. C. Paris, and A. A. Wells (1967). Basic aspect of crack growth and fracture, Chap. 7 in Technology of steel pressure vessels for water-cooled nuclear reactors. G. D. Whitman, G. C. Robinson, Jr., A. W. Savolainen (Eds.), USAEC Rep. ORNL-NSIC-21, 430-538.
- Kamada, A., N. Koshizuka, and T. Funakoshi (1976). Effect of austenite grain size and C content on the substructure and toughness of tempered martensite and bainite. Trans. ISIJ, 16, 407-416.
- Kotilainen, H. (1979). The temperature dependence of the fracture toughness and the cleavage fracture strength of a pressure vessel steel. ASTM, 12th Nat. Symp. on Fracture Mechanics, (St. Louis).
- Kotilainen, H. (1980). To be published.
- Kotilainen, H., K. Törrönen, and P. Nenonen (1980). The influence of microstructure on the fracture toughness of a bainitic steel. Analytical and Experimental Fracture Mechanics, (Rome).
- Malkin, J., and A. S. Tetelman (1971). Relation between  $K_{Ic}$  and microscopic strength for low alloy steels. Eng. Fract. Mech., 3, No. 2, 151-167.
- Nakazawa, K., and G. Krauss (1978). Microstructure and fracture of 52100 steel. Met. Trans., 9A, 681-689.
- Naylor, J. P. (1979). The influence of the lath morphology on the yield stress and transition temperature of martensitic-bainitic steels. Met. Trans. A, 10A, 861-873.
- Rice, J. R., and M. A. Johnson (1970). The role of large crack tip geometry changes in plane strain fracture. In H. F. Kanninen and co-workers (Ed.), Inelastic Behaviour of Solids, McGraw-Hill, New York, 641-670.
- Rice, J. R., and G. F. Rosengren (1968). Plane strain deformation near a crack tip in a power-law hardening material. J. Mech. Phys. Solids, 16, 1-12.
- Ritchie, R. O., J. F. Knott, and J. R. Rice (1973). On the relationship between critical tensile stress and fracture toughness in mild steel. J. Mech. Phys. Solids, 21, 395-410.
- Ritchie, R. O., W. L. Server, and R. A. Wullaert (1979). Critical fracture stress and fracture strain models for the prediction of lower and upper shelf toughness in nuclear pressure vessel steels. Met. Trans. A, 10A, No. 10, 1557-1570.
- Roesch, L. (1973). Influence of second-phase particles on the low-temperature fracture behaviour of iron. Proc. 3rd Int. Conf. on Fracture (Munich), Vol. IV, III-344.
- Roman, I., C. A. Rau, Jr., A. S. Tetelman, and K. Ono (1979). Fracture and fatigue properties of 1Cr-Mo-V bainitic turbine rotor steels. EPRI Tech. Rep. NP-1023 Research Project 700-1, (Palo Alto), 1-222.

- Tanaka, J., S. Tani, and C. Ouchi (1975). Low temperature toughness of water-cooled and tempered low carbon manganese steel. Trans. ISIJ, 15, (1), 19-26.
- Tetelman, A. S., T. R. Wilshaw, and C. A. Rau, Jr. (1968). The critical tensile stress criterion for cleavage. Int. J. Fract. Mech., 4, No. 2, 147-157.
- Törrönen, K. (1979). Microstructural parameters and yielding in a quenched and tempered Cr-Mo-V pressure vessel steel. Tech. Res. Centre of Finland, Materials and Processing Technology, Publication 22, 1-106.
- Tracey, D. M. (1976). Finite element solutions for crack-tip behavior in small-scale yielding. J. Eng. Mat. and Techn. Trans. ASME, 146-151.
- Wobst, K., and D. Aurich (1977). Assessment of flaws in structural components on the basis of a hypothesis for cleavage fracture. Proc. 4th Int. Conf. on Fracture (Waterloo), D. M. R. Taplin (Ed.), Univ. of Waterloo Press, 2, 183-193.
- Yaroshevich, V. D., and D. G. Ryvkina (1970). Thermal-activation nature of plastic deformation in metals. Sov. Phys.-Solid State, 12, No. 2, 363-370.